

Supporting information

Laser-fabricated sandwiched fog collector enabling agricultural irrigation and electricity generation

Xinran Dong^{1#}, Jinghui Gao^{1#}, Yan Zhang¹, Yuxin Song^{2*}, Longhui Huang¹, Hong Luo¹,
Xiongfeng Zhou¹, Cong Wang³, Ji-an Duan³, and Minjie Liu⁴

¹College of Mechanical and Intelligent Manufacturing, Central South University of Forestry and Technology, 498 South Shaoshan Street, Changsha 410004, China

²Department of Mechanical Engineering, The Hong Kong Polytechnic University, Hung Hom, Kowloon, Hong Kong, 100872, China

³State Key Laboratory of Precision Manufacturing for Extreme Service Performance, College of Mechanical and Electrical Engineering, Central South University, 932 South Lushan Street, Changsha, 410083, China

⁴School of Mechanical Engineering, Tiangong University, 399 Binshui West Road, Tianjin 300387, China

#These authors contributed equally: Xinran Dong, Jinghui Gao;

*Corresponding author: yxsong6@outlook.com

This file includes

Supplementary Figure S1-9.....	2
Supplementary Table S1-2.....	11
Supplementary Video S1-2	13

Supplementary Figure S1-7

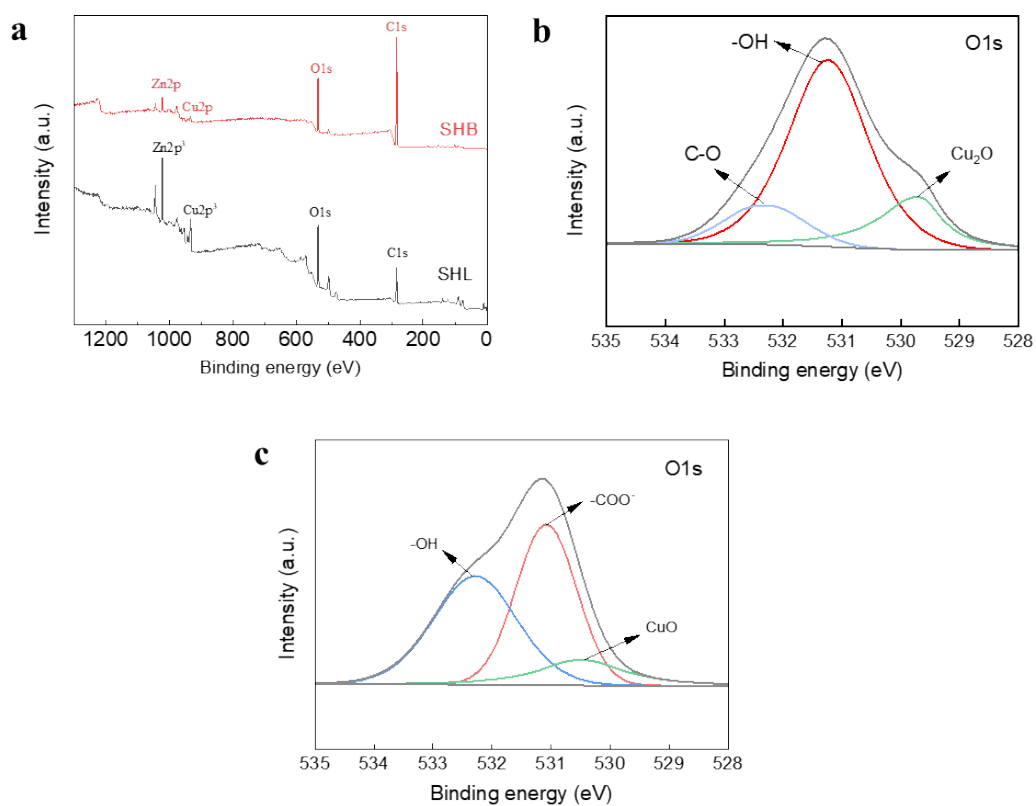


Figure S1. (a) XPS spectrums of the SHL and SHB meshes. (b) High-resolution XPS spectrum of O1s for the SHL mesh. (c) High-resolution XPS spectrum of O1s for the SHB mesh.

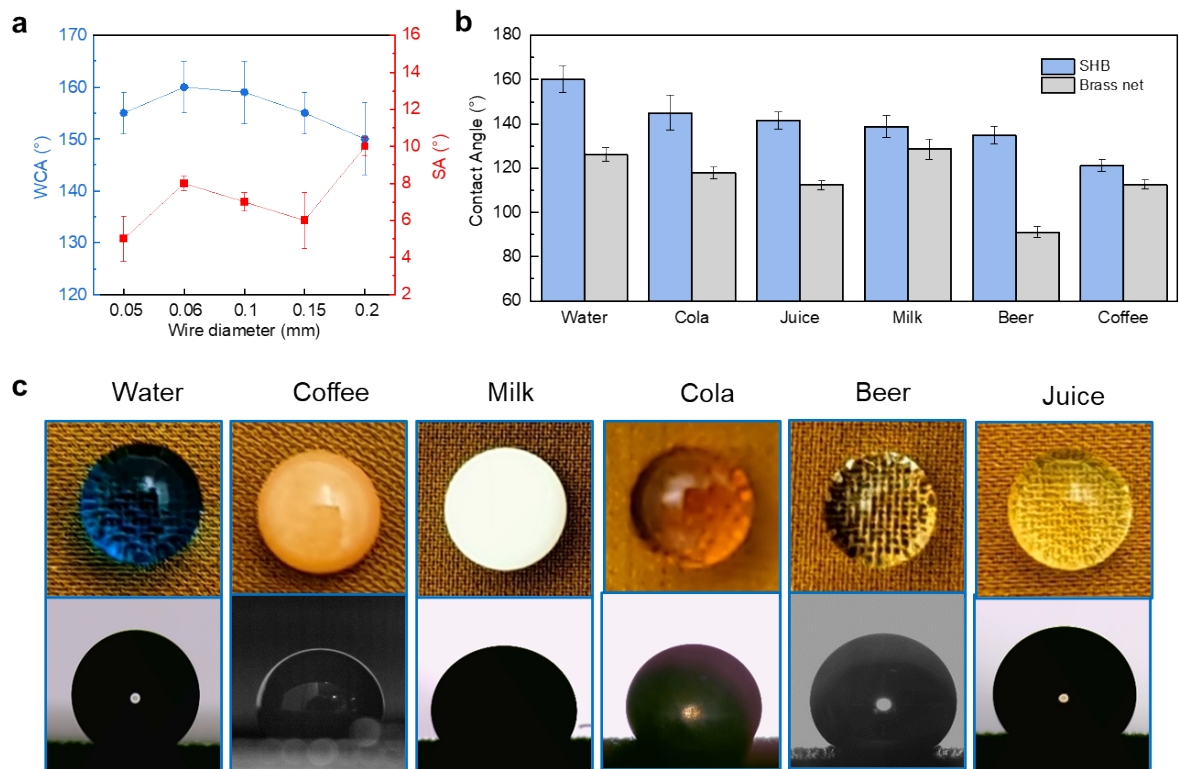


Figure S2. (a) Water contact angles (WCAs) and sliding angles (SAs) of the SHB meshes with different wire diameters. (b) Contact angles of different liquids on the SHB mesh. (c) Optical images of different liquids on the SHB mesh.

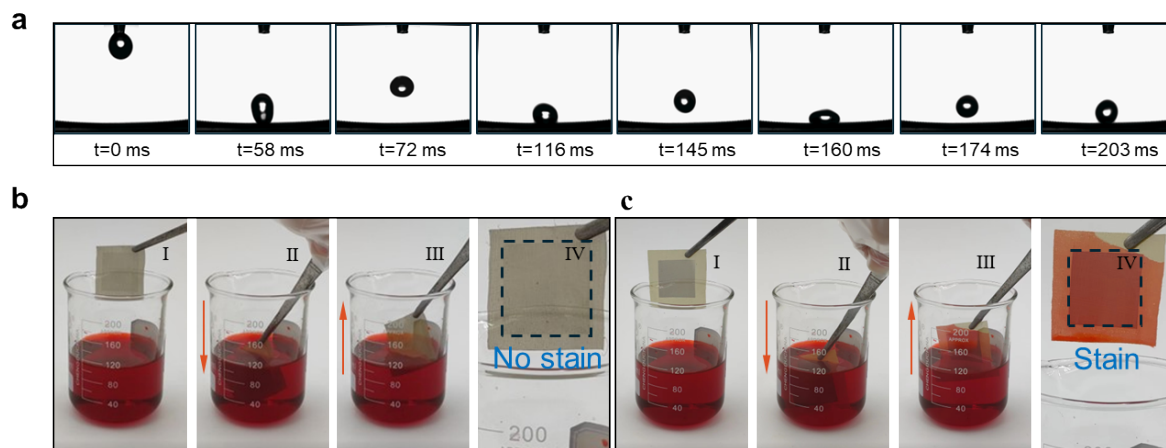


Figure S3. (a) Dynamics of droplet rebound on the SHB mesh. (b) Water soaking tests of SHL mesh. (c) Water soaking tests of SHB mesh.

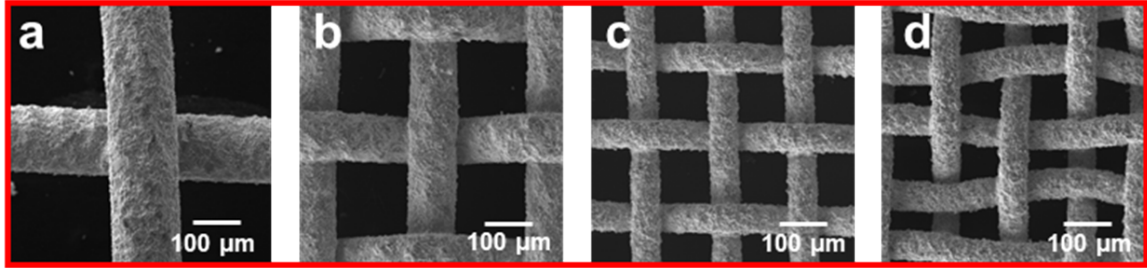


Figure S4. SEM images of meshes with different wire diameters (a) 0.15 mm (Mesh number: 50), (b) 0.10 mm (Mesh number: 100), (c) 0.06 mm (Mesh number: 150), (d) 0.05 mm (Mesh number: 200).

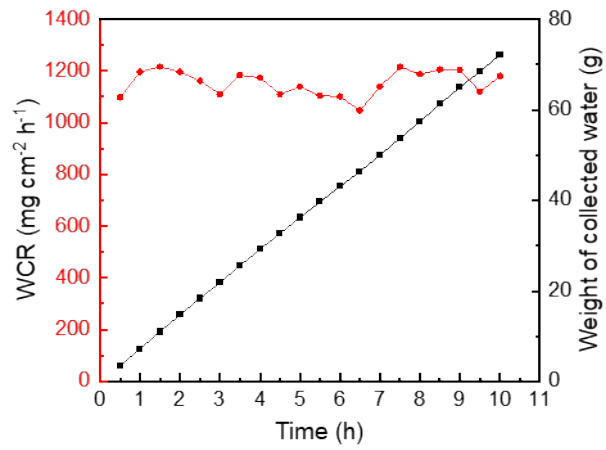


Figure S5. Water collection rate (WCR) and weight of collected water of the large-scale sandwiched fog collector.

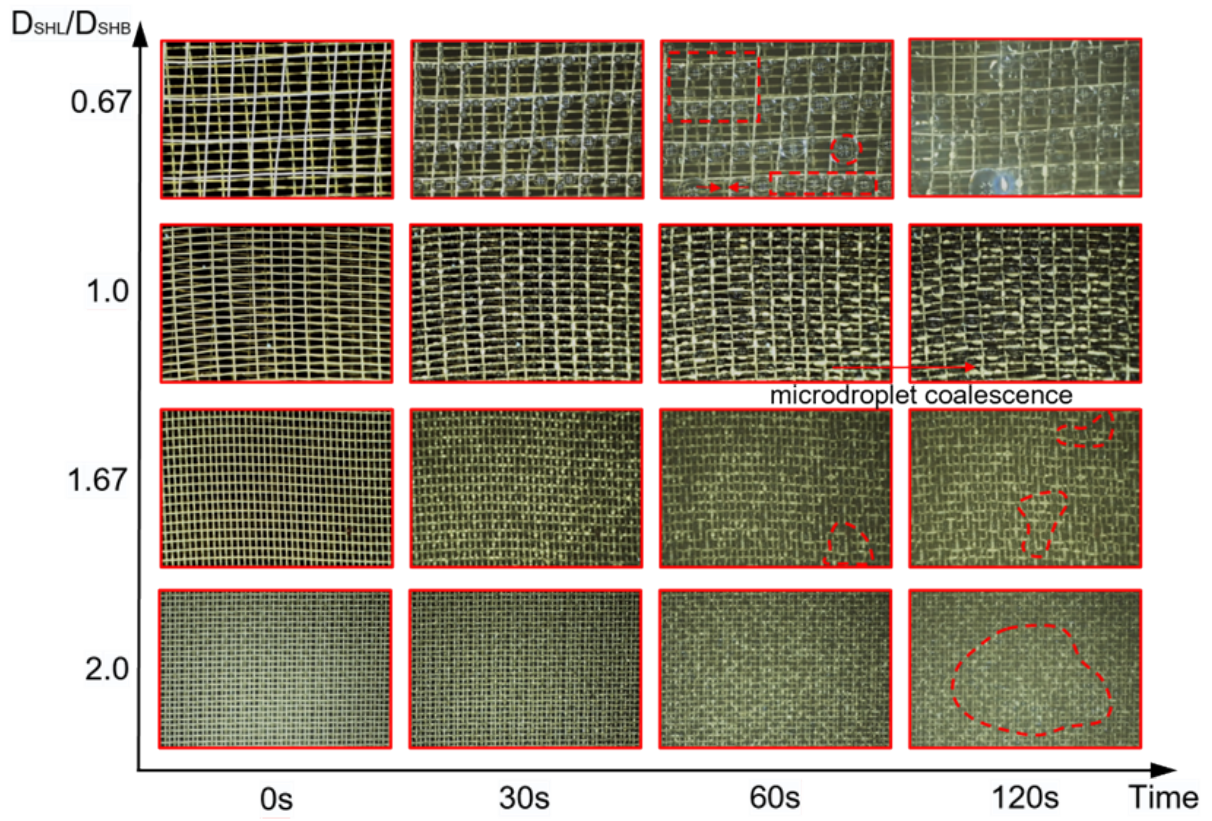


Figure S6. Droplet penetration behavior of samples with varying D_{SHL}/D_{SHB} ratios

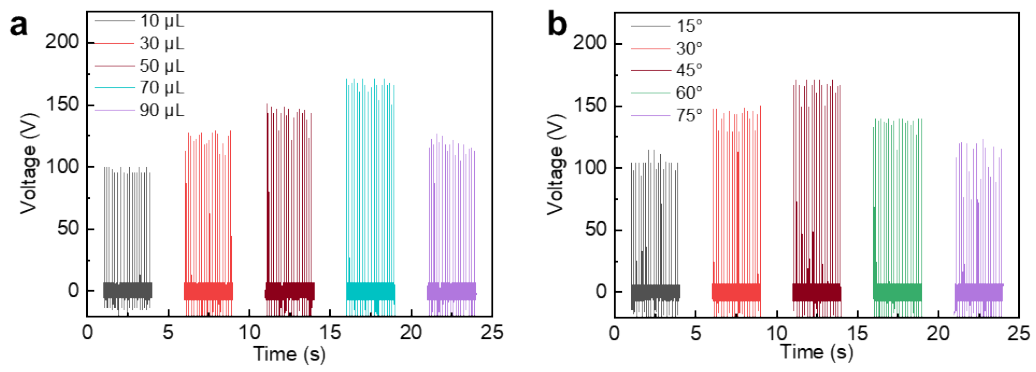


Figure S7. (a) Output voltage of the DEG impacted by droplets with different volume. (b) Output voltage of the DEG with different tilt angles.

Supplementary Table S1-2

Table S1 The corresponding relationship between the wire diameter and mesh number

Mesh number	Wire diameter (mm)
20	0.20
50	0.15
100	0.10
150	0.06
200	0.05

Table S2 Comparison of different fog collectors

Layers	Materials	Airflow transmission	Configurations	Airflow volume	WCR ($\text{mg}\cdot\text{cm}^{-2}\cdot\text{h}^{-1}$)	References
				(ml/h)/Flow velocity (cm/s)/RH/TEMP		
1	Copper	Impermeable	Hybrid surfaces	280/-/95%/27°C	110.7	[27]
1	PDMS	Impermeable	Large-area SHB surfaces	-/-/-	159	[28]
1	Ti	Impermeable	SHB hierarchical surfaces	312.12/-/28%/-	543.4	[29]
1	Glass	Impermeable	SHL/SHB patterned surfaces	180/-/80%/20°C	916.8	[26]
1	Steel mesh	Permeable	Wettability-patterned meshes	-/1.02/54%/24°C	177.65	[32]
1	Alloy wires	Permeable	Bio-inspired topological alloy net	-/0.45/90%/25°C	1050	[31]
1	PTFE	Permeable	3D vertical filament mesh	350/15/90%/23°C	28.76	[30]
1	Wire meshes	Permeable	Fog harps	141/15/100%/room temperature	~3000	[7]
2	PTFE sheet/Copper mesh	Impermeable	Hybrid surface	-/10/-/20°C	200	[11]
3	Polyester mesh	Permeable	Sandwiched Janus nets	-/100/60%/25°C	370	[21]
3	Brass mesh	Permeable	Sandwiched brass nets	150/40/50%/25°C	1200	Our work

Supplementary Video S1-2

Video S1 Droplet transfer from the SHB mesh to SHL mesh.

Video S2 A fluent airflow pathway of the sandwiched fog collector.